

This is an Open Access document downloaded from ORCA, Cardiff University's institutional repository: <https://orca.cardiff.ac.uk/id/eprint/116659/>

This is the author's version of a work that was submitted to / accepted for publication.

Citation for final published version:

Kanitkar, Swarom, Carter, James H., Hutchings, Graham J., Ding, Kunlun and Spivey, James J. 2018. Low temperature direct conversion of methane using a solid superacid. *ChemCatChem* 10 (21), pp. 5033-5038. 10.1002/cctc.201801310

Publishers page: <http://dx.doi.org/10.1002/cctc.201801310>

Please note:

Changes made as a result of publishing processes such as copy-editing, formatting and page numbers may not be reflected in this version. For the definitive version of this publication, please refer to the published source. You are advised to consult the publisher's version if you wish to cite this paper.

This version is being made available in accordance with publisher policies. See <http://orca.cf.ac.uk/policies.html> for usage policies. Copyright and moral rights for publications made available in ORCA are retained by the copyright holders.

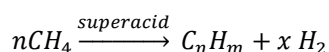


Supporting Information

Low Temperature Direct Conversion of Methane using a Solid Superacid

Swarom Kanitkar,^[a] James Carter,^[b] Graham Hutchings,^[a,b] Kunlun Ding,^[a] James J Spivey,^{*[a]}

Abstract: The direct conversion of methane to higher hydrocarbons and hydrogen can be catalyzed using “superacids”:



The first report of catalytic oligomerization of methane using superacids was that of Olah et al., who demonstrated the superacidity of FSO_3H-SbF_5 , which is a liquid. More recently, Vasireddy et al. showed that gas-phase $HBr/AlBr_3$ was an active superacid. The only reported solid superacid for methane oligomerization is sulfated zirconia (SZ). Here, we report a new class of Br-based solid superacids, $AlBr_x/H-ZSM-5$ (“ABZ-5”, $x=1$ or 2). ABZ-5 is based on the gas-phase $HBr/AlBr_3$, with the objective of synthesizing a heterogeneous analogue of the gas-phase superacid $HBr/AlBr_3$. The results show that ABZ-5 is significantly more active than SZ. Perhaps more significantly, results showed methane conversions of $\sim 1\%$ at $300^\circ C$ using ABZ-5, while the lowest temperature reported in the literature is $350^\circ C$. Here, we demonstrate direct conversion of methane using a solid superacid catalyst, $AlBr_x/H-ZSM-5$. This solid catalyst is synthesized using a vapor-phase process in which $AlBr_3$ vapor is grafted on to solid H-ZSM-5. This catalyst is characterized using NH_3 -TPD, XRD, and FTIR. Hydrocarbon products observed in the temperature range of $200 - 400^\circ C$ include both C_2 - C_6 hydrocarbons and aromatics.

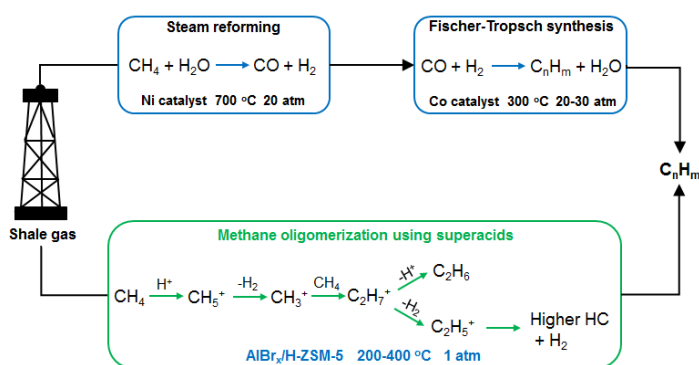


Figure 1. Current and proposed process for converting methane into olefins and fuels. At present, methane is reformed into syngas and then transformed into higher hydrocarbons through the Fischer-Tropsch synthesis. This indirect process requires high temperatures and pressures. Methane oligomerization using solid superacids offers a direct route to converting methane into higher hydrocarbons under mild conditions.

[a] M.S.-Chem. Eng., S. Kanitkar, Dr. K. Ding, Dr. J. J. Spivey, Dr. G. Hutchings
Cain Department of Chemical Engineering
Louisiana State University
Baton Rouge, LA – 70803, USA
E-mail: hutch@cardiff.ac.uk

[b] Dr. J. Carter, Dr. G. Hutchings
Cardiff Catalysis Institute
Cardiff University
Cardiff, UK CF10 3AT

Table of Contents

1. Materials and Methods.....	3
2. Results and Discussion.....	3
2.1 Catalyst preparation.....	4
2.2 Thermodynamics.....	4
2.3 XRD	5
2.4 DRIFTS	6
2.5 Reaction runs	9
3. References.....	9

1. Materials and Methods

A schematic for a reaction system is shown in Figure S1.

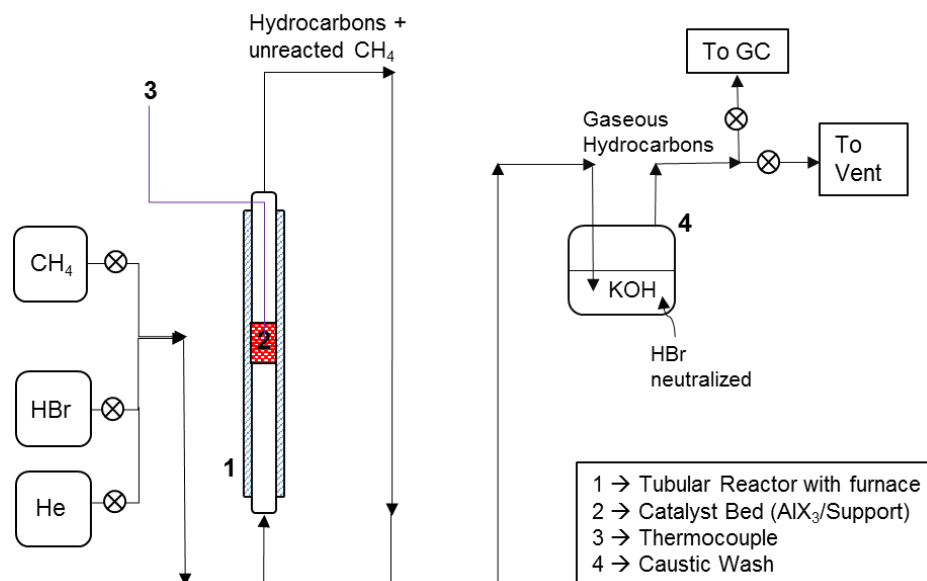
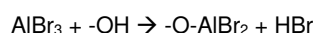


Figure S1: Schematic for CH₄ reaction system

From the NH₃-TPD calculations (Table 3, main text) and the calculations for gain in weight after grafting, it was observed that roughly 80 % of the Al sites formed through grafting were active for NH₃ adsorption and thus were used in the TOF calculation (shown below). Another assumption that was made was the species on the surface of H-ZSM-5 are -AlBr₂ with one Br losing through the reaction with hydroxyl group as shown below:



An example calculation is as shown below:

Weight of H-ZSM-5 (before grafting) = 1.40 g,

Weight of ABZ-5 (AlBr₃ grafted H-ZSM-5) = 1.53 g.

Difference in weight = 0.13 g

Molecular weight of -AlBr₂ = 189 g/mol → moles of AlBr₂ grafted = 0.13 g/189 g.mol⁻¹ = 0.000688 mol AlBr₂

Moles of Al = 0.000688 mol/1.53 gcat = 0.000449 mol.gcat⁻¹

Difference in acidity from NH₃-TPD = 1556 μmol.gcat⁻¹ - 1190 μmol.gcat⁻¹ = 366 μmol.gcat⁻¹

So 0.000449 mol Al adsorbed 366 μmol NH₃ → 1 mol Al adsorbed ~ 0.82 mol of NH₃

This calculation was used in calculating TOF and thus 80% of Al sites were assumed to be active.

2. Results and Discussion

The grafting of AlBr₃ on H-ZSM-5 was confirmed by several means: (a) gain in weight of the zeolite after grafting, (b) the apparent color change from white to skin (also confirmed using UV-Vis), (c) capturing the HBr gas generated during grafting in deionized water and checking for the change in pH before and after grafting. In the (c) test, the water pH became acidic side and the specific gravity of the water increased, consistent with the capture of HBr. Finally, a silver nitrate (AgNO₃) test was also carried out on the water sample on the captured HBr. The test was positive, indicating that bromine was captured. Collectively, these tests confirm the reaction between AlBr₃ and surface hydroxyls of H-ZSM-5, forming the grafted AlBr_x/H-ZSM-5 complex.

It was also attempted to characterize the grafting using FTIR, Raman spectroscopy. However, analytical capabilities of FTIR limited the inorganic bonds with vibrations in the far-IR region that are not within the standard range available on all IR spectrometers. With the Raman, excessive fluorescence from sample prevented from obtaining any meaningful spectra of these catalysts.

There were other limitations in using X-ray edge techniques. For example, overlapping of 'Br' L edge peaks with 'Al' K edge peaks that prevented quantification of the elements using EDX (Energy Dispersive X-ray) spectroscopic technique. Further, ²⁷Al MAS NMR could not distinguish between the Al from the H-ZSM-5 framework and the Al from AlBr₃ grafting, because the contribution from Al in H-ZSM-5 was too large.

Hammett indicators are often employed to measure the superacidity of solid catalysts. However, the Hammett indicator technique is typically based on a color change from basic to acidic upon addition of the solid catalyst in the indicator solution. This technique works well with the white powders that do not change the color of the indicator solution on its own^[1]. However, in the present case, the

catalysts were already colored so the Hammett indicator technique could not be employed for assessing the acidity/superacidity of the present catalysts.

Another test of of superacidity of catalysts acidity in the literature is the isomerization of butane to isobutane at room temperature [2]. However, in the case of H-ZSM-5, butane appears to be trapped inside the zeolite pores at low concentrations at temperatures < 100 °C. Only if the catalyst is heated to temperatures > 100 °C, butane appears to be desorbed and could be analyzed using FID. However, carrying out the reaction of butane to isobutane at elevated temperature is often claimed not to be a true measure of superacidity [2-3].

2.1 Catalyst preparation

Table S1 describes the physico-chemical properties of the main catalyst of interest here. Base H-ZSM-5 had a measured surface area of 435 m²/g that decreased to 380 m²/g after the AlBr₃ grafting (ABZ-5). This indicates that AlBr₃ was grafted on to H-ZSM-5. Spent ABZ-5 after the reaction at 300 °C had a surface area of 422 m²/g that shows a slight drop from the H-ZSM-5 but a higher surface area than ABZ-5. This could have been due to two opposite mechanisms: bromine loss would result in increase in surface area than ABZ-5, while deposition of coke that would decrease the surface by blocking the pores. If so, the net effect is a slight decrease of surface area compared to the H-ZSM-5.

Table S1: Physico-chemical properties of the catalysts

Catalyst	BET surface area (m ² /g)	Al content through XPS (at%)	Br content through XPS (at%)	Br content through AgNO ₃ test (wt%)
H-ZSM-5	435	1.15	-	-
Fresh ABZ-5	380	0.98	0.06	2.29
Spent ABZ-5*	422	0.94	0.04	1.43

* Spent Catalyst – ABZ-5 recovered after CH₄ oligomerization at 300 °C, 1 atm, 9 L.gcat⁻¹hr⁻¹ for 16 hrs

Although, Al 'K edge' and Br 'L edge' are very close as mentioned before, due to low concentrations of Al and Br, XPS allowed to see two distinct peaks separated by 1-2 eV. Surface aluminum and bromine concentrations could thus be obtained and it could be confirmed that the loss of bromine occurred during the reaction and is also supported by AgNO₃ test. Difference in bromine contents from XPS and AgNO₃ could be attributed to the nature of the techniques: surface vs. bulk.

ICP-OES analysis was attempted in order to calculate Al content of the samples of interest. However, we had difficulties in complete digestion of these samples through lithium metaborate fusion and microwave assisted HF digestion could not be performed due to safety issues.

2.2 Thermodynamics

In the case of halide-based catalysts, often the possibility of formation of methyl halide (CH₃X) is considered. However, based on the thermodynamic calculations (using HSC Chemistry 8.6) under the presence of AlBr_x species, the thermodynamic extent of CH₃Br formation from CH₄ is negligible. Typically formation of these species (CH₃Br) requires the presence of a stronger oxidant such as Br₂ that are able to generate significant quantities [4].

Methane conversions at the temperatures of interest here, range from 0.5 – 12 % (Table S2) depending on whether coke formation is allowed/not allowed. Figure S2 shows a comparison of CH₄ conversion at various temperatures from 25 °C to 1000 °C with and without coke formation is allowed.

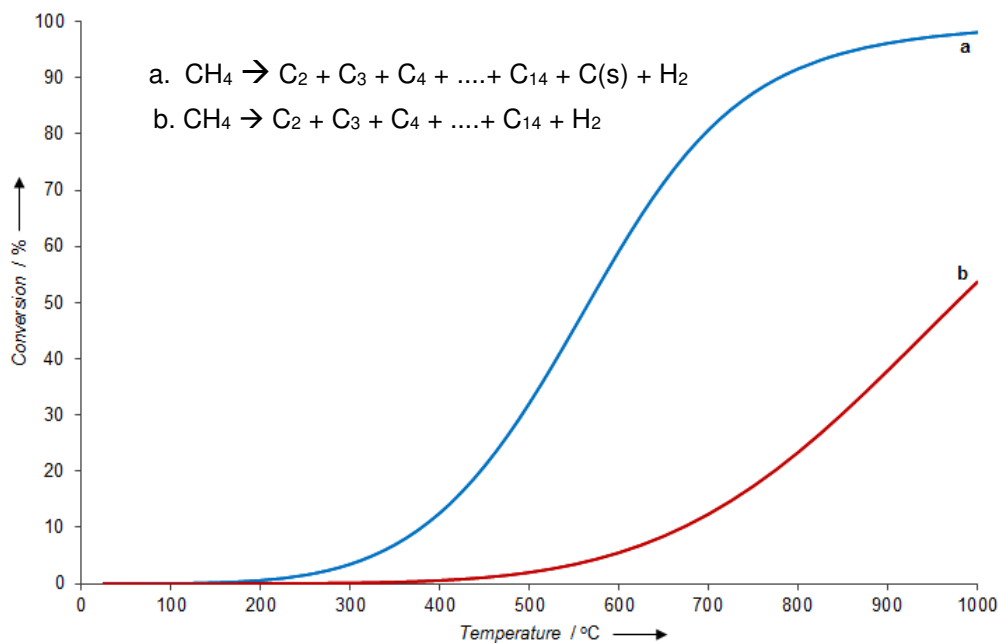


Figure S2: Thermodynamic CH_4 conversion against temperature (a) with coke formation allowed, (b) without coke formation allowed (calculated using HSC Chemistry 8.6)

Table S2: Thermodynamic CH_4 conversion versus temperature with and without coke formation allowed

Temperature (°C)	CH ₄ conversion (%)	
	w/o coke	w/coke
25	0	0.002
100	0.002	0.04
200	0.023	0.577
300	0.118	3.463
400	0.558	12.57

2.3 XRD

Figure S3 shows a comparison between H-ZSM-5 sample, fresh AlBr_3 grafted H-ZSM-5 (ABZ-5) sample, and spent ABZ-5 sample. All three spectra show the characteristic peaks of H-ZSM-5. When compared based H-ZSM-5 (a) and fresh ABZ-5 (b), XRD shows no extra features arising from the grafting of AlBr_3 . This indicates that AlBr_x species are well dispersed and no long-range order exists. Further no measurable difference between fresh and spent catalyst (b, c; respectively) could be seen indicating no structural change in the base zeolite H-ZSM-5 during the reaction, as expected due to low reaction temperatures (200- 400 °C) of interest here.

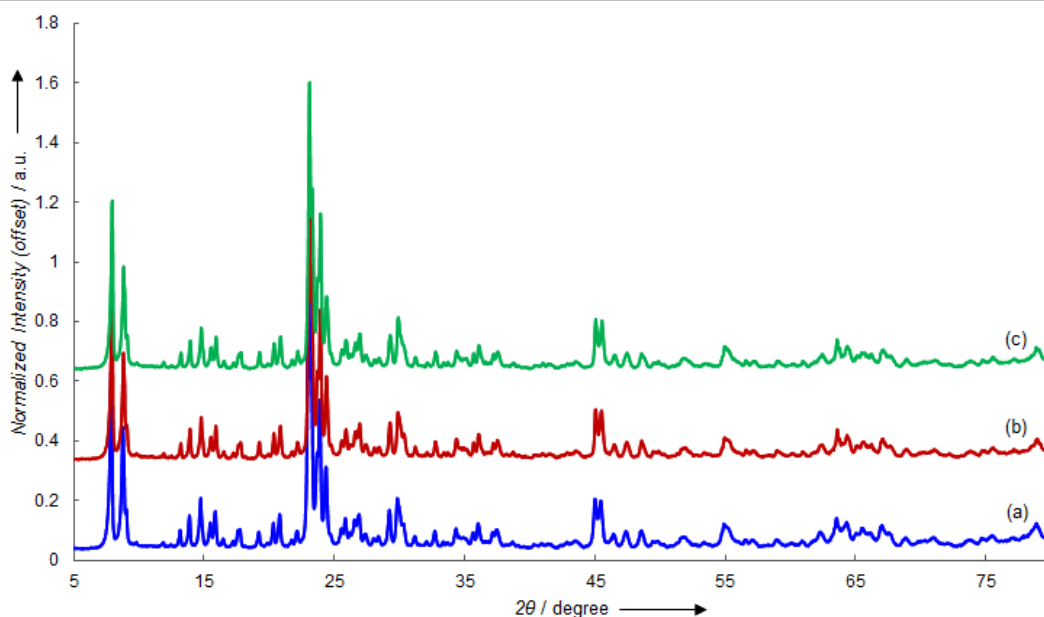
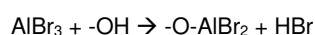


Figure S3: XRD comparison of (a) H-ZSM-5, (b) Fresh ABZ-5, (c) Spent ABZ-5

2.4 DRIFTS

It is known that three type of hydroxyls^[5] are present on H-ZSM-5: one that is attached to both Al, Si (Al-OH-Si), one being attached only to Si- commonly known as silanols (Si-OH), and the third one being non-framework hydroxyls. Al-OH-Si hydroxyl groups are the acidic ones having IR vibration band $\sim 3610 \text{ cm}^{-1}$, silanols are the terminal $-\text{OH}$ groups with IR vibration $\sim 3740 \text{ cm}^{-1}$, while the non-framework hydroxyls show bands around $3670 - 3690 \text{ cm}^{-1}$. Figure S4 shows the IR spectrum for H-ZSM-5 and ABZ-5 catalyst in the $-\text{OH}$ group region from $3600\text{-}3700 \text{ cm}^{-1}$. It can be observed for both H-ZSM-5 and ABZ-5, that there exists three IR bands in the $-\text{OH}$ region (3580 cm^{-1} , 3650 cm^{-1} , 3740 cm^{-1}) that can be attributed to acidic hydroxyl, non-framework hydroxyls, and silanols. When AlBr_3 was grafted on the H-ZSM-5, we observed a decrease in the intensity of the band around 3740 cm^{-1} corresponding to the silanol group. This is consistent with the hypothesis that Br atoms from AlBr_3 react with $-\text{OH}$ groups on the surface of H-ZSM-5. Similar decrease in the intensity of peaks corresponding to silanol has been observed when AlCl_3 was grafted on siliceous MCM-41^[6]. This decrease in the intensity is most likely due to occurrence of the following reaction:



Thermal stability of the acid sites on the most active catalyst, ABZ-5 was also tested using pyridine-DRIFTS. Spectra for ABZ-5 catalyst after pyridine desorption at temperatures up to $400 \text{ }^\circ\text{C}$ are shown in Figure S5. Both Lewis and Brønsted acid sites are present on this catalyst at room temperature. Along with bands for these acids sites, there are bands that correspond to hydrogen bonded pyridine at $\sim 1600 \text{ cm}^{-1}$. As the temperature is increased, as expected, bands corresponding to hydrogen bound pyridine start decreasing, as do the bands corresponding to the Lewis acid site. On the contrary, Brønsted acid sites appear to be stable at all temperatures.

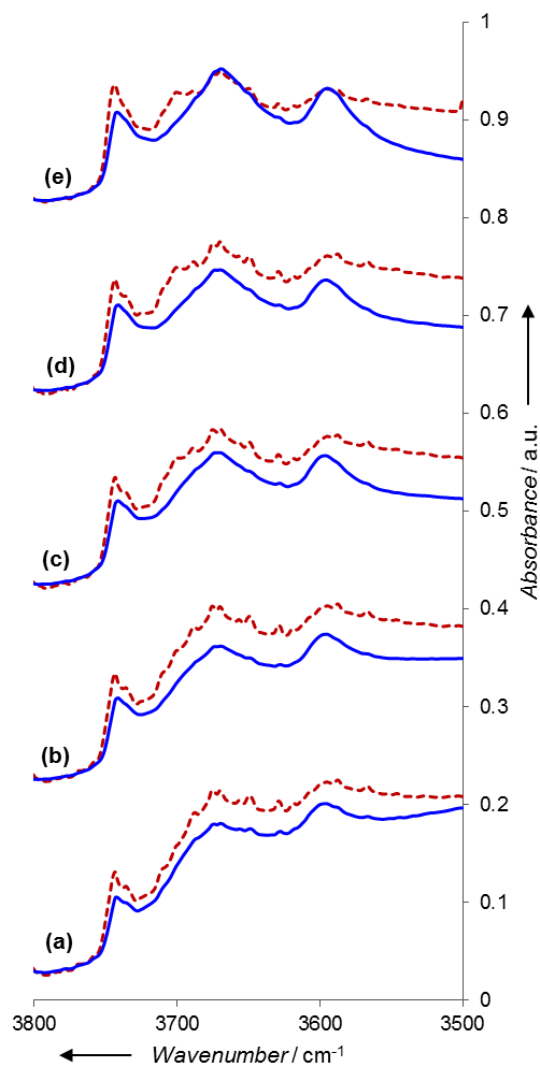


Figure S4: IR spectra for hydroxyl group region for H-ZSM-5 (dotted) and ABZ-5 (undotted), (a) at 25 °C, (b) at 100 °C, (c) at 200 °C, (d) at 300 °C, (e) at 400 °C

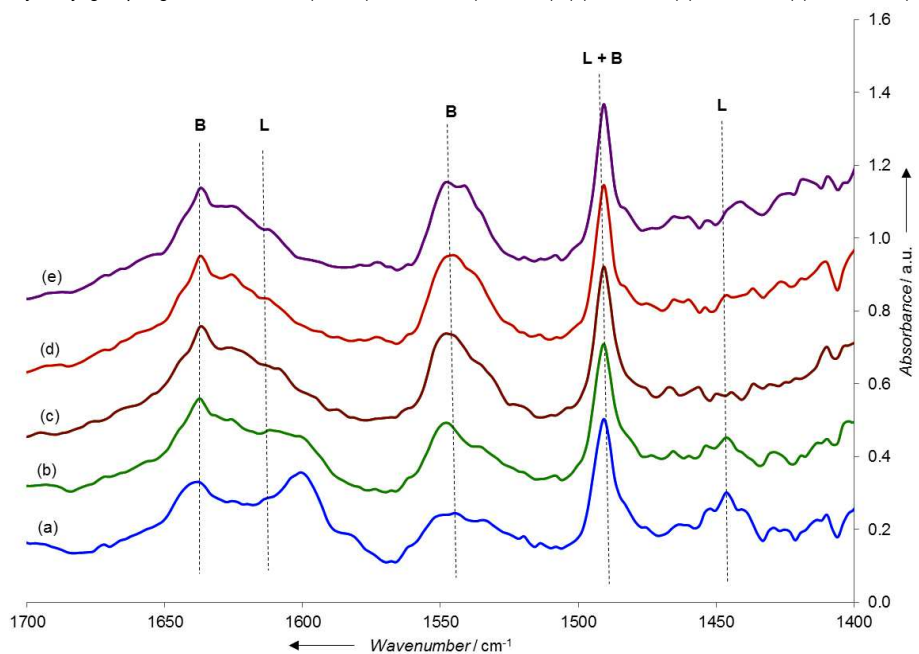


Figure S5: DRIFTS spectra for ABZ-5 catalyst after pyridine desorption at (a) 25 °C, (b) 100 °C, (c) 200 °C, (d) 300 °C, (e) 400 °C

Figure S6 and Figure S7 also show stable acid sites of both type (L and B) up to high temperatures ~ 400 °C for catalysts: Sulfated Zirconia as well as base H-ZSM-5 respectively. Although strength of the acid sites must be stronger in the case ABZ-5 compared to these two catalysts.

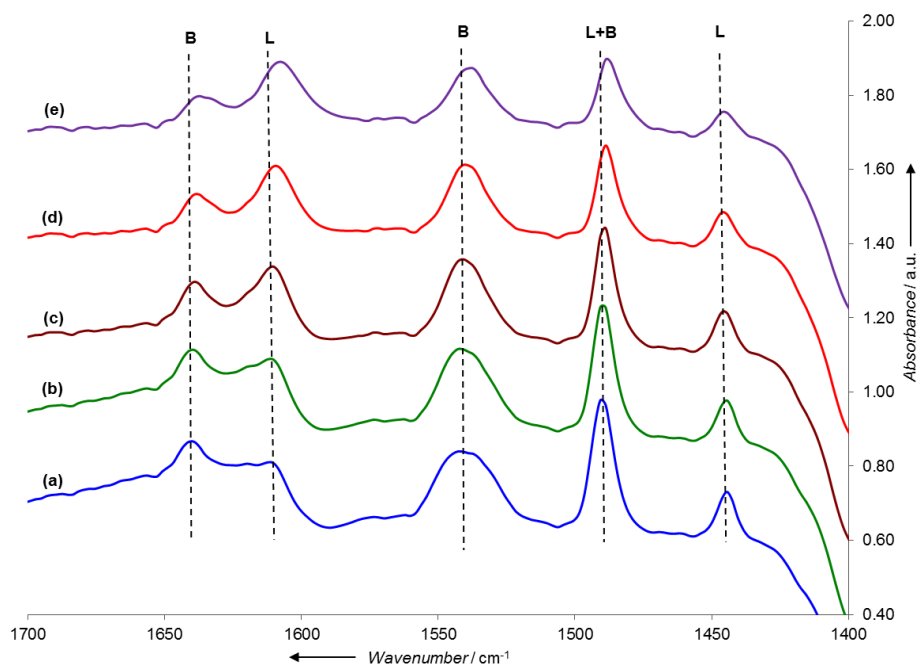


Figure S6: DRIFTS spectra for SZ catalysts after pyridine desorption at (a) 25 °C, (b) 100 °C, (c) 200 °C, (d) 300 °C, (e) 400 °C

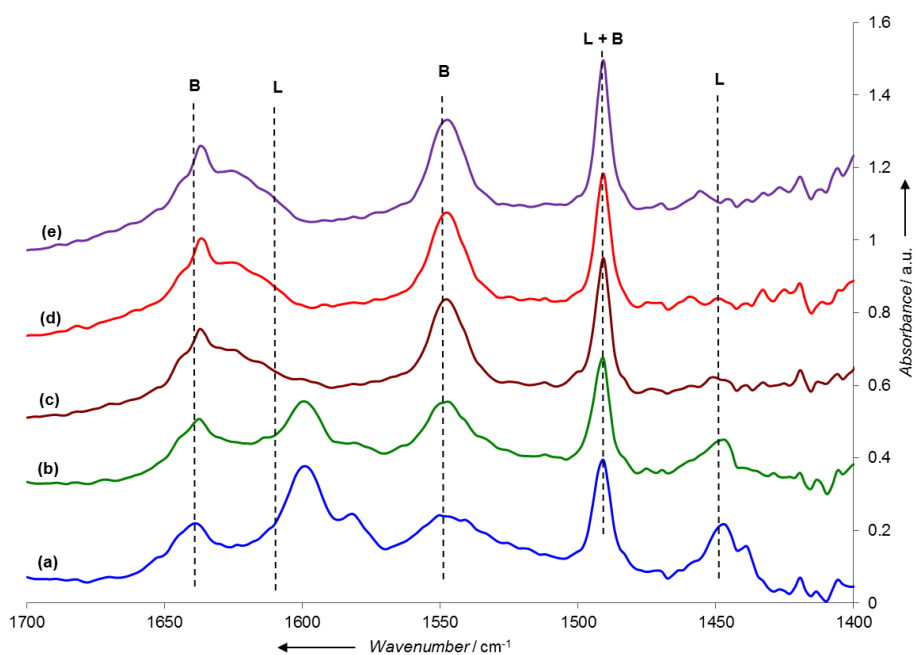


Figure S7: DRIFTS spectra for H-ZSM-5 catalysts after pyridine desorption at (a) 25 °C, (b) 100 °C, (c) 200 °C, (d) 300 °C, (e) 400 °C

A comparison at 300 °C for H-ZSM-5 versus ABZ-5 (Figure 2a, main manuscript) shows that both the spectra are very similar, except for a small shoulder at 1540 cm^{-1} that is present in the case of ABZ-5 and not in H-ZSM-5. We believe that this could have been due to grafting of AlBr_3 on H-ZSM-5 creating a new Brønsted acid site.

Table S3: Area under the curve for pyridine DRIFTS

Catalyst	Area under curve (acid sites)
----------	-------------------------------

	L (1450 cm ⁻¹)	L+B (1490 cm ⁻¹)	B (1540 cm ⁻¹)	L (1620 cm ⁻¹)	B (1640 cm ⁻¹)
H-ZSM-5	-	3.07	4.53	2.57	3.23
Fresh ABZ-5	-	3.69	5.63	3.06	4.03
Spent ABZ-5	-	1.17	1.37	-	0.50

It is known that DRIFTS is not a quantitative technique [7] and often transmission is the most commonly used technique for quantification. We thus did not attempt to quantify acid sites based on these results. However, based on just the area under curve (Table S3), that more pyridine adsorbed on the fresh ABZ-5 catalyst than H-ZSM-5, supporting the hypothesis that there are more acid sites on fresh ABZ-5 than base H-ZSM-5. When spent ABZ-5 was also tested using pyridine DRIFTS, area under the curve was clearly very less, indicating less access to the acid sites possibly due to blocking of the pores by coke formation and due to loss of 'Br'.

2.5 Reaction runs

To avoid the ambiguity of whether the activity originated from H-ZSM-5 or purely due to AlBr₃ doping, H-ZSM-5 was subjected to further analysis. At 300 °C, no significant hydrocarbon peaks were observed for H-ZSM-5, indicating no activity. However, when the same H-ZSM-5 is tested at 400 °C, low levels of oligomerization products are detected, as shown in Table S4, but the concentration is much lower compared to those formed on the ABZ-5 catalyst. Additionally, after 2 h on-stream, only trace amounts of C₂–C₅ hydrocarbons were detected.

Table S4: Time on stream (TOS) of CH₄ oligomerization on H-ZSM-5 at 400 °C, 9 L gact⁻¹h⁻¹, 1 atm. (-) = not detected

Time (hr)	TOF (h ⁻¹)	Product selectivity (%)							
		C ₂₌	C ₃	C ₄	C ₅	B	T	EB	X (o,m,p)
1	0.002	49.1	-	-	-	11.2	31.9	-	7.9
2	-	99.9	-	-	-	-	-	-	-
3	-	99.9	-	-	-	-	-	-	-
Blank	-	-	-	-	-	-	-	-	-

To calculate the TOF in these (and subsequent) runs, both the methane conversion rate and a valid value for the number of superacid sites are needed. In the experiments discussed here, the conversion of methane is measured by the difference between the inlet concentration (5% from a high-purity tank) and the outlet concentration, both measured using a GC/MSD ("Reaction Studies" above). Detection limits for the hydrocarbon analytes of interest here are 0.1 ppm in these experiments, which makes it difficult to accurately estimate the methane conversion values (e.g. 5 % vs. 4.99 %), considering the uncertainties associated with even slight fluctuations in flow controllers, catalyst weights, temperature of the reaction. In addition, the superacid sites may differ at different temperatures. Thus, here in the present results, we do not report methane conversion values. This, and because methane conversions are typically closer to 1%, a single value for the TOF at all reaction conditions is not possible, even if reaction conditions change slightly. We find that in the literature of superacid methane oligomerization, TOF is often not reported, presumably due to the uncertainties associated with these experiments.

In terms of detecting hydrogen, TCD is most often used. However, detecting low concentrations of hydrogen is extremely difficult as TCD relies heavily on the difference in thermal conductivities, which should be large for a detectable signal. In the present case, the differences between the inlet and outlet concentration would be ~ 50 – 100 ppm, which was clearly far below the detection limits on the analytical instruments used here, and thus although hydrogen is produced, it could not be quantified.

Attempts for direct conversion of methane have been reported in the literature over to over solid superacids, in particular using sulfated zirconia catalysts. Rezgui et al. [8], Hua et al. [9], Martin and Schmal [10] observed primarily C₂ hydrocarbons (mostly ethane). Hydrogen was observed, indicating an oligocondensation mechanism similar to the one proposed by Olah for liquid superacids [11], although others did not report any hydrogen, possibly due to scavenging of oxygen by the dihydrogen [12] or due to incorporation into the carbonaceous deposits [8].

3. References

- [1] G. A. Olah, G. K. Surya Prakash, Á. Molnár, J. Sommer, in *Superacid Chemistry*, John Wiley & Sons, Inc., **2009**, pp. 1-34.
- [2] V. Adeeva, H.-Y. Liu, B.-Q. Xu, W. H. Sachtler, *Topics in Catalysis* **1998**, *6*, 61-76.
- [3] J. R. Sohn, *J. Ind. Eng. Chem.* **2004**, *10*, 1-15.
- [4] K. Ding, H. Metiu, G. D. Stucky, *ACS Catalysis* **2013**, *3*, 474-477.
- [5] H. Berndt, A. Martin, H. Kosslick, B. Lücke, *Microporous Materials* **1994**, *2*, 197-204.
- [6] V. R. Choudhary, K. Mantri, *Journal of Catalysis* **2002**, *205*, 221-225.
- [7] T. Armaroli, T. Bécue, S. Gautier, *Oil & Gas Science and Technology - Rev. IFP* **2004**, *59*, 215-237.
- [8] S. Rezgui, A. Liang, T. K. Cheung, B. C. Gates, *Catalysis Letters* **1998**, *53*, 1-2.
- [9] W. Hua, A. Goepfert, J. Sommer, *Applied Catalysis A: General* **2001**, *219*, 201-207.
- [10] R. L. Martins, M. Schmal, *Applied Catalysis A: General* **2006**, *308*, 143-152.

-
- [11] G. A. Olah, Y. Halpern, J. Shen, Y. K. Mo, *Journal of the American Chemical Society* **1973**, *95*, 4960-4970.
[12] D. Fraenkel, *Catalysis Letters* **1999**, *58*, 123-125.